Efficient Analysis of Parameter Uncertainty in FDTD Models of Microwave Circuits using Polynomial Chaos

Andrew C. M. Austin and Costas D. Sarris

The Edward S. Rogers Sr. Department of Electrical and Computer Engineering

University of Toronto, Ontario, Canada M5S 3G4

email: acm.austin@ieee.org

Abstract—**An FDTD-based model is developed to analyze three dimensional microwave circuits with uncertain parameters, such as variability and tolerances in the physical dimensions introduced by manufacturing processes. The proposed method uses generalized polynomial chaos to expand the time-domain electric and magnetic fields in terms of orthogonal polynomial basis functions of the uncertain variables. The technique is validated by modelling a low pass microstrip filter with uncertain stub lengths. The computed S-parameters are compared against Monte Carlo simulations, and good agreement is found for the statistics over 0–20 GHz. A considerable computational advantage over the Monte Carlo method is also achieved.**

Index Terms—**Uncertainty, Finite difference methods, Monte Carlo methods.**

I. INTRODUCTION

Computational electromagnetic tools, such as the finite-difference time-domain (FDTD) method, are widely used to design microwave circuits. However, uncertainties introduced in the manufacturing processes are difficult to capture using existing computational methods [1]. For example, manufacturing tolerances introduce uncertainty in the physical dimensions, which 'propagates' through the circuit to induce uncertainty in the response. Characterizing the randomness in the circuit response is an essential step in the design and validation process to estimate the sensitivity of the predictions and for setting realistic design margins [2].

The Monte Carlo method is widely used to quantify the impacts of uncertainty and randomness in numerical models, and has been demonstrated to provide accurate results for electromagnetic problems [3]. However, statistics computed via the Monte Carlo method generally converge slowly, and this tends to limit its application for computationally large or complex problems. Other methods, such as perturbation with truncated series expansions can also be used for sensitivity and uncertainty analysis. However, perturbation is usually only valid for small changes in the input parameters [4].

Recently, methods based on generalized polynomial chaos have been proposed to more efficiently quantify large-scale uncertainty in numerical models [4]. The polynomial chaos method approximates quantities in a stochastic process as the finite summation of orthogonal basis polynomials in the random input parameter space [4]. While the computational costs are increased, relative to the non-stochastic case, polynomial chaos techniques converge significantly faster than the Monte Carlo method, and can provide estimates for the uncertainties
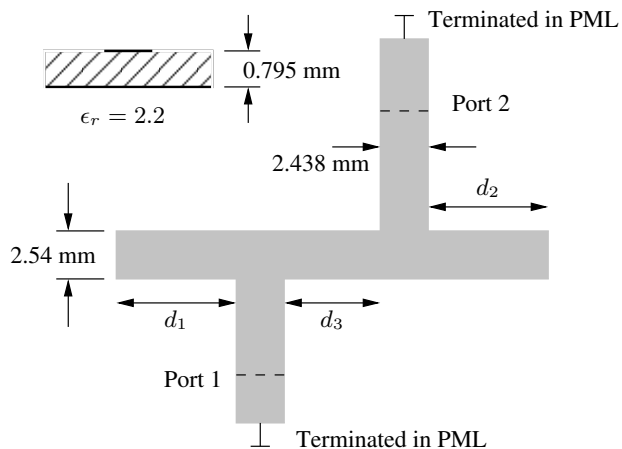

Fig. 1. Microstrip implementation of a low pass filter with uncertain dimensions: $d_1 = 5.69 \pm 0.5$ mm; $d_2 = 5.69 \pm 0.5$ mm; and $d_3 = 4.064 \pm 1.0$ mm. Other dimensions are assumed to remain constant.

and sensitivities from a single simulation run. Previous applications of polynomial chaos for microwave circuits have not focused on full-wave simulation methods—these have examined the effects of statistical variability in the per-unit-length parameters for single- and multi-conductor transmission lines using the telegrapher's equations [2]. Meanwhile, FDTD-based implementations of the polynomial chaos method have largely focused on the analysis of loaded resonant cavities and free-space scattering problems [5].

The results presented in this paper demonstrate the flexibility and strength of the polynomial chaos method, when combined with full-wave computational electromagnetic techniques, to characterize the effects of parameter uncertainty in practical microwave circuits. Also considered is the concurrent estimation of the parameter sensitivities via the Sobol decomposition [6]. Furthermore, polynomial chaos provides a mathematical framework for potentially incorporating multi-resolution analysis in the uncertain parameter space using expansions in other orthogonal bases, such as wavelets.

II. UNCERTAINTY IN THE FDTD ANALYSIS

Fig. 1 shows a microstrip implementation of a 5.6 GHz low pass filter, with three uncertain dimensions identified, $\{d_1, d_2, d_3\}$. These uncertainties can be expressed as random variables, with the actual dimensions viewed as a particular realization [4]. It is assumed the random dimensions are statistically independent and follow uniform probability distributions. In this analysis, the random dimensions are

incorporated into the FDTD method by introducing uncertainty in the cell spacing of the rectilinear Yee lattice. For example, the uncertainty in the Δx lattice spacing, due to stub length d_1, can be expressed by

$$\Delta x(\xi_1) = \frac{\Delta x^{\max} + \Delta x^{\min}}{2} + \frac{\Delta x^{\max} - \Delta x^{\min}}{2}\xi_1, \quad (1)$$

where ξ_1 is a uniformly distributed random variable over the interval $-1 \le \xi_1 \le 1$, and $\Delta x^{\min}$ and $\Delta x^{\max}$ represent the minimum and maximum values of the lattice spacing required to achieve the desired uncertainty in d_1. The uncertainty in the lattice spacing is distributed over a region to reduce spurious numerical reflections from the interface. Similarly, to ensure numerical stability the time-step is reduced to account for the smallest possible cell dimension.

A. The Polynomial Chaos Expansion

Uncertainty in the computational lattice dimensions will introduce uncertainty in the time-domain electric and magnetic fields throughout the problem space. The polynomial chaos method expands these uncertain fields as a truncated summation of orthogonal polynomial basis functions, Ψ_l, in the N random variables, $\boldsymbol{\xi} = \{\xi_1, \ldots \xi_N\}$ [5]. For example, the E_z field component can be written

$$E_z\big|_{i,j,k+\frac{1}{2}}^n(\boldsymbol{\xi}) = \sum_{l=0}^{P} e_z^l\big|_{i,j,k+\frac{1}{2}}^n \Psi_l(\boldsymbol{\xi}). \quad (2)$$

The number of terms is given by $P + 1 = \frac{(N+D)!}{N!D!}$, where D is the highest polynomial order in the expansion. For the uniformly distributed stub lengths considered in this paper, basis functions from the set of Legendre polynomials are used. Other orthogonal basis functions, such as wavelets, could also be applied to more efficiently span the random parameter space. The Legendre basis functions are orthogonal over an $\Omega = [-1, 1]^N$ probability space, with an inner product given by

$$\langle \Psi_l \Psi_m \rangle = \int_\Omega \Psi_l \Psi_m \, d\boldsymbol{\xi} = \langle \Psi_m^2 \rangle \delta_{l,m}. \quad (3)$$

Similar expressions to (2) can be formulated for the remaining electric and magnetic field components and substituted into the FDTD update equations along with (1). The E_z update equation can be expressed

$$\sum_{l=0}^{P} e_z^l\big|_{i,j,k+\frac{1}{2}}^{n+1} \Psi_l(\boldsymbol{\xi}) = \frac{2\epsilon_0\epsilon_r - \sigma\Delta t}{2\epsilon_0\epsilon_r + \sigma\Delta t} \sum_{l=0}^{P} e_z^l\big|_{i,j,k+\frac{1}{2}}^{n} \Psi_l(\boldsymbol{\xi})$$
$$+ \frac{2\Delta t}{2\epsilon_0\epsilon_r + \sigma\Delta t}\left[\sum_{l=0}^{P} \frac{h_y^l\big|_{i+\frac{1}{2},j,k+\frac{1}{2}}^{n+\frac{1}{2}} - h_y^l\big|_{i-\frac{1}{2},j,k+\frac{1}{2}}^{n+\frac{1}{2}}}{\Delta x(\boldsymbol{\xi})} \Psi_l(\boldsymbol{\xi})\right.$$
$$\left. - \sum_{l=0}^{P} \frac{h_x^l\big|_{i,j+\frac{1}{2},k+\frac{1}{2}}^{n+\frac{1}{2}} - h_x^l\big|_{i,j-\frac{1}{2},k+\frac{1}{2}}^{n+\frac{1}{2}}}{\Delta y(\boldsymbol{\xi})} \Psi_l(\boldsymbol{\xi})\right]. \quad (4)$$

Applying a Galerkin procedure by taking inner products with the test function $\Psi_m(\boldsymbol{\xi})$, where $m = 0, \ldots P$, and using the

orthogonality condition from (3), reduces (4) to

$$e_z^m\big|_{i,j,k+\frac{1}{2}}^{n+1} = \frac{2\epsilon_0\epsilon_r - \sigma\Delta t}{2\epsilon_0\epsilon_r + \sigma\Delta t} e_z^m\big|_{i,j,k+\frac{1}{2}}^{n} + \frac{2\Delta t}{2\epsilon_0\epsilon_r + \sigma\Delta t}\cdot$$
$$\frac{1}{\langle \Psi_m^2 \rangle}\left[\sum_{l=0}^{P}\left(h_y^l\big|_{i+\frac{1}{2},j,k+\frac{1}{2}}^{n+\frac{1}{2}} - h_y^l\big|_{i-\frac{1}{2},j,k+\frac{1}{2}}^{n+\frac{1}{2}}\right)\left\langle\frac{\Psi_l(\boldsymbol{\xi})\Psi_m(\boldsymbol{\xi})}{\Delta x(\boldsymbol{\xi})}\right\rangle\right.$$
$$\left. - \sum_{l=0}^{P}\left(h_x^l\big|_{i,j+\frac{1}{2},k+\frac{1}{2}}^{n+\frac{1}{2}} - h_x^l\big|_{i,j-\frac{1}{2},k+\frac{1}{2}}^{n+\frac{1}{2}}\right)\left\langle\frac{\Psi_l(\boldsymbol{\xi})\Psi_m(\boldsymbol{\xi})}{\Delta y(\boldsymbol{\xi})}\right\rangle\right]. \quad (5)$$

The inner products in (5) are precomputed using numerical quadrature and stored in memory before time-stepping commences. Where there is no uncertainty in the cell dimensions the inner products reduce to Kronecker delta functions, and the $m = 0, \ldots P$ update equations are decoupled. The FDTD computational lattice is terminated in a 10-cell thick perfectly matched layer (PML); these regions are free of parameter uncertainty, and the PML can be applied to each $m = 0, \ldots P$ field component separately.

The global sensitivity of the circuit response to each stub length can be estimated using the Sobol decomposition of the polynomial chaos expansion. This yields a set of conditional variances, indicating the relative contribution each combination of input parameters makes toward the uncertainty in the response. The Sobol indices for the set of inputs u are given by

$$S_u = \frac{\sum_{m \in K_u} (e_z^m)^2 \langle \Psi_m^2 \rangle}{\sum_{m=1}^{P} (e_z^m)^2 \langle \Psi_m^2 \rangle}, \quad (6)$$

where K_u is an index to the terms in (2) that contain u [6].

III. Numerical Results

The FDTD computational lattice for the microstrip filter depicted in Fig. 1 is $130 \times 100 \times 36$ cells in size (including the PML), and the nominal cell dimensions are: $\Delta x = 0.4064$ mm; $\Delta y = 0.4233$ mm and $\Delta z = 0.265$ mm [7]. The filter is excited at port 1 using a modulated Gaussian pulse with a 10 GHz centre frequency and solved to 4000 time steps. The Monte Carlo method is applied by generating a set of 1000 uniformly distributed random dimensions, appropriately scaling the lattice spacing, and solving each realization of the circuit independently. Changes to the stub lengths alters the frequency-domain response of the filter, including the magnitude of the ripple in the pass- and stop-bands and the roll-off. Fig. 2(a) shows the mean S_{21} magnitude computed using Monte Carlo simulations and the FDTD polynomial chaos formulation outlined in section II-A. The corresponding standard deviation about the mean values is shown in Fig. 2(b). The standard deviation is observed to increase in the roll-off regions of the filter response, indicating an increased degree of uncertainty exists in the results at these points.

The polynomial chaos expansion is truncated at order $D = \{1, 2, 3\}$, and the uncertainty in the time-domain e_z^m field components (recorded at ports 1 and 2) is projected into the frequency-domain to determine the S-parameter statistics. As
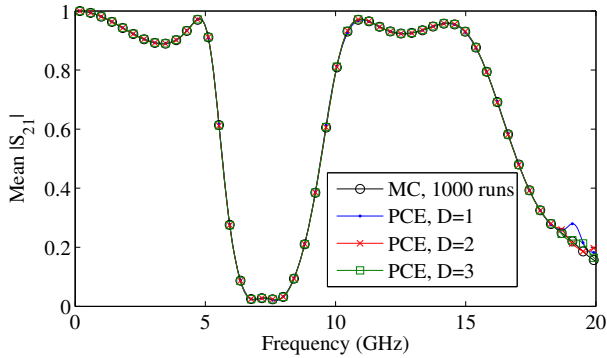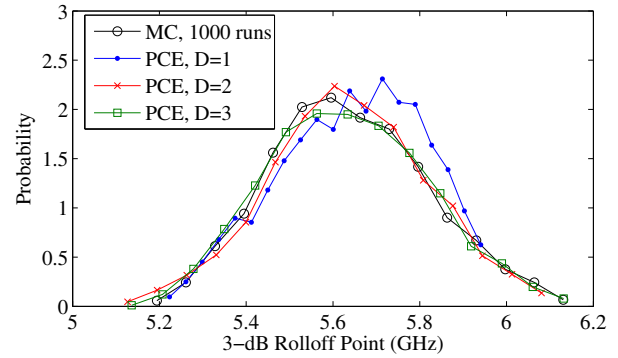
(a)
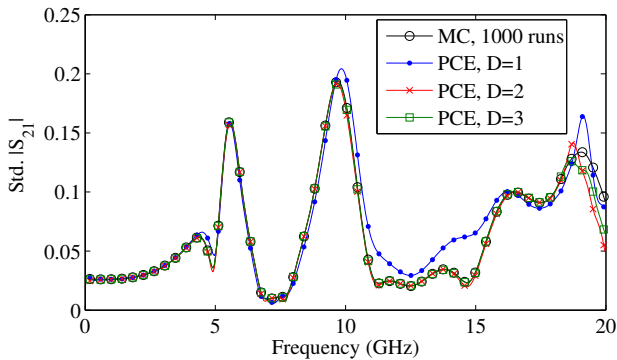
(b)

Fig. 2. Comparison of the (a) Mean and (b) Standard deviation in the magnitude of filter S_{21} computed using 1000 Monte Carlo trials and via polynomial chaos expansions.

(a)

(b)

Fig. 3. (a) Probability density functions of the low pass filter 3-dB roll-off point computed using 1000 Monte Carlo trials and via polynomial chaos expansions. (b) Relative contribution of each stub length to the uncertainty in $|S_{21}|$ computed using the $D = 3$ expansion.
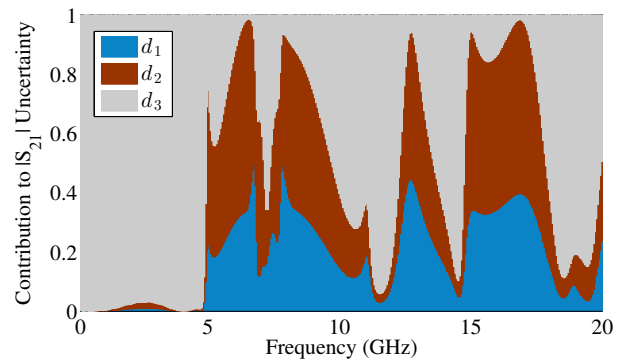
shown in Fig. 2(a) and (b), the mean and standard deviation are well predicted, and the convergence against the Monte Carlo results improves with increasing D. At higher frequencies the change in the electrical lengths of the stubs is larger, causing increased uncertainty, which requires higher order polynomial terms to converge.

Fig. 3(a) shows PDFs of the 3-dB filter roll-off frequency estimated from 1000 Monte Carlo trials and via the polynomial chaos expansions. Accurate models for the expected spread are important to assess the sensitivity of the predictions, and can provide a measure of confidence in simulated results. Increasing the order of the expansion improves the shape of the distribution, though further Monte Carlo trials would be required to improve accuracy in the tails. Fig. 3(b) shows the relative contribution of each stub length to the uncertainty in $|S_{21}|$ computed via (6). The uncertainty in the pass band ripple is dominated by d_3, the stub separation; whereas in the transition regions and the stop band, the lengths of the stubs have greater impact. This analysis is valuable as it indicates which parameters should be targeted to have the greatest reduction in the variability of the response.

The simulation time for each Monte Carlo trial is approximately 4 minutes (on a 3.3 GHz Intel i3 processor); 1000 trials thus takes 2.5 days. By comparison, the polynomial chaos method requires approximately 8, 23 and 58 minutes for $D = 1$–3 respectively. However, the overall memory

consumption is increased by factor $P + 1$, which may limit its application for electrically large problem geometries.

IV. CONCLUSIONS

Randomness in the physical dimensions of microwave circuits, e.g. manufacturing tolerances, introduces uncertainty in the response. Characterizing this uncertainty using numerical simulation tools is advantageous, but often requires excessive computational resources. The model developed in this paper uses polynomial chaos to introduce uncertainty in the 3D FDTD method. The method is applied to determine the effects of uncertainty in the dimensions of a microstrip filter. The statistics of the solution agree closely with Monte Carlo results and are achieved at significantly lower computational cost.

REFERENCES

[1] L. R. A. X. de Menezes, A. O. Paredes, H. Abdalla, and G. A. Borges, "Modeling device manufacturing uncertainty in electromagnetic simulations," in *Digest IEEE MTT-S Int. Microw. Symp.*, 2008, pp. 1385–1388.

[2] P. Manfredi and F. G. Canavero, "Polynomial chaos-based tolerance analysis of microwave planar guiding structures," in *Digest IEEE MTT-S Int. Microw. Symp.*, 2011, pp. 1132–1136.

[3] F. Hastings, J. Schneider, and S. Broschat, "A Monte-Carlo FDTD technique for rough surface scattering," *IEEE Trans. Antennas Propag.*, vol. 43, no. 11, pp. 1183–1191, 1995.

[4] D. Xiu and G. Karniadakis, "The Wiener-Askey polynomial chaos for stochastic differential equations," *SIAM J. Sci. Comput.*, vol. 24, no. 2, pp. 619–644, 2002.

[5] R. S. Edwards, A. C. Marvin, and S. J. Porter, "Uncertainty analyses in the finite-difference time-domain method," *IEEE Trans. Electromagn. Compat.*, vol. 52, no. 1, pp. 155–163, Feb. 2010.

[6] T. Crestaux, O. Le Maitre, and J.-M. Martinez, "Polynomial chaos expansion for sensitivity analysis," *Reliab. Eng. Syst. Safe.*, vol. 94, no. 7, pp. 1161–1172, 2009.

[7] D. Sheen, S. Ali, M. Abouzahra, and J. Kong, "Application of the three-dimensional finite-difference time-domain method to the analysis of planar microstrip circuits," *IEEE Trans. Microw. Theory Tech.*, vol. 38, no. 7, pp. 849–857, 1990.